UDC 544.137/.537:666.652

E. Kim[1, *], Y. Shimotsuma[1, **], M. Sakakura[2], K. Miura[1]
[1]Department of Material Chemistry, Graduate School of Engineering, Kyoto University, Kyoto, Japan
[2]Next Generation Laser Processing Technology Research Association, Kyoto, Japan
**eunhokim@func.mc.kyoto-u.ac.jp*
***yshimo@func.mc.kyoto-u.ac.jp*

Nano periodic structure formation in 4H–SiC crystal using femtosecond laser double-pulses

The photo-induced periodic nano structure inside 4H–SiC have been induced by a femtosecond double pulse train. The alignment of the periodic structure is in the direction independently from crystal orientation. In particular, FE-SEM analysis revealed that the periodic structure on the fractured surface can be classified into two categories of the polarization-dependent and polarization-independent.

***Keywords**: 4H–SiC, periodic nano structure, femtosecond laser, double pulse, phase change, semiconductor.*

INTRODUCTION

Among the wide bandgap semiconductors, SiC is very hard material and has excellent properties such as high breakdown voltage and thermal/chemical stability. Therefore, it is expected as a key material for next generation power devices. On the other hand, SiC is also known as a hardly processed material because of high hardness property. Recently, the conventional wire-saw slicing technique is employed to fabricate semiconductor wafer from ingot [1–4]. Such technique also employed for SiC wafer, which has advantages for mass production from its high throughput [5]. The other approach of smart cut method using proton also proposed to settle some negative issues for SiC substrate [6–8]. At the recent time, a stealth dicing method has been used to cut the fabricated semiconductor device chip on the wafer using an ultrashort pulse laser [9–11], this dicing technique has also attractive to improve the production for SiC applications [12, 13]. In recent years, material modification using ultrashort pulse laser has attracted attention because there is possibility of applying it with potential photonic application. The structural changes induced by femtosecond laser pulses have been studied about various transparent bulk materials at wavelength from visible to NIR ranging from glass [14, 15], diamond [16], TeO_2 [17], ZnO [18], GaN [19], 4H–SiC [20], GaP [21], Si [22]. In the case of SiC, the formation of the nano voids due to micro-explosion and periodic structure has been reported [20]. It is known that periodic nano structures can be formed in indirect semiconductors or dielectric, and their arrangement direction is divided vertical [15, 17] or horizontal [20–22] with respect to the polarization direction of light. The dominant mechanism on the dependence of the arrangement direction in the polarization direction is still not clear. Therefore, we elucidated the mechanism of periodic structure formation by investigating 4H–SiC more in detail from previous research.

[20] In this study, we investigated the modified structure in the 4H–SiC using femtosecond pulse laser with double pulse train technique [23]. We confirmed that the periodic nano structure is aligned not only depend on the polarization direction of the light but also in the scanning direction as a circular shape regardless of single- and double-pulse-trains with strong fluence rather than previous report. Moreover, the periodic nano structure also aligned in the polarization direction without depending on the crystal orientation.

EXPERIMENTAL

In the study, we used commercially available nitrogen-doped 4H–SiC (0001) wafer with a thickness of 420 μm (Tankeblue semiconductor). We prepared two types of samples, a 5×5 mm square chip cut from wafer for *c*-plane (0001), and a 0.4×5 mm rectangular rod using *c*-plane chip in which vertically set up then polished it by CMP method for *a*-plane (11 $\bar{2}$ 0). The detail procedure of laser-slicing method was described our previous report. [23] The experiments were carried out using femtosecond laser oscillator equipped with a regenerative amplifier (Cyberlaser; IFRIT) The center wavelength, pulse duration (τ_{pulse}) and pulse repetition rate of this laser system were 780 nm, 220 fs and 1 kHz, respectively. The schematic illustration of 4H–SiC crystal structure and irradiation direction is shown in Fig. 1.

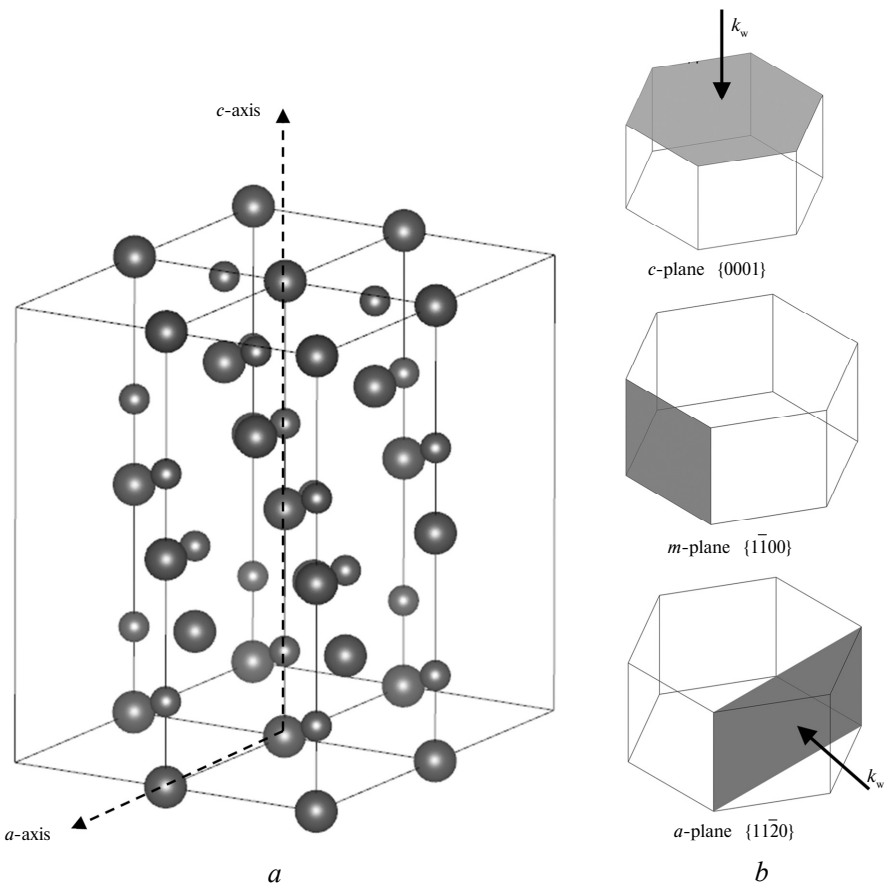

Fig. 1. Crystal structure of 4H–SiC (*a*), main crystal planes of *c*- , *m*-, *a*-plane (*b*).

To investigate the optimal condition for (11 $\bar{2}$ 0), the τ_{pulse} was changed from 220 fs to 1 ps. Moreover, to enhance the light-matter interaction, we configured the Mach-

Zehnder type of double pulse optical setup [24]. The time delay (τ_{delay}) between femtosecond double pulses was controlled by using an optical delay line. The total pulse energy (E_{pulse}) of the equally divided double pulses was tuned by neutral density filter. To compensate the spherical aberration due to the high refractive index of SiC (n_0 = 2.6 at λ = 780–800 nm), we used a spatial light modulator (LCOS-SLM, Hamamatsu Photonics; X10468). The pre-calculated CGH for the correction of spherical aberration at the focal depth of 260 μm was displayed on LCOS-SLM. The laser beam was focused inside a SiC wafer with a 50× objective (Nikon, LU Plan Fluor; NA 0.80, Transmittance ≈ 80 % at 800 nm). Since we have compensated the spherical aberration, the beam diameter obtained to be approximately 1.2 μm. To reveal the orientation dependence of the periodic structure, the laser pulse was induced SiC inside sample to the [0001] (*c*-plane) or [11 $\bar{2}$ 0] (*a*-plane) directions. The typical laser energy before objective lens was to be 10 μJ, a typical laser fluence was calculated to be 5.7×10^2 J/cm^2. The absorption coefficient of 4H–SiC at 780 nm was set to be 26 cm^{-1} for *c*-plane and 47 cm^{-1} for *a*-plane, respectively [25]. The laser-written tracks at a spacing of 25 μm in the SiC wafer were typically formed by scanning the wafer relative to the focus at 100 μm/s with direction to {11 $\bar{2}$ 0}. After laser writing, the samples were fractured off in the plane perpendicular to the laser-written tracks using instant glue on the sample surfaces and SUS-holding locking jig. The fractured surface morphology was characterized by FE-SEM (JEOL; JSM-6705F). To reveal the detailed structural changes by the laser writing, the observation by using an aberration corrected high resolution transmission electron microscope (JEOL; JEM-2200FS) was performed.

RESULTS AND DISCUSSIONS

Threshold for (11 $\bar{2}$ 0) SiC Crystal Internal Laser-Processing

In order to optimize the laser-processing condition for *a*-plane, we investigated the damage threshold by using single- or double-pulse trains with different E_{pulse}. The polarization of electric field is set to parallel to the *c*-axis. In the case of single pulse train, we were unable to modifying or impossible to processing the *a*-plane inside even if the pulse duration increasing until 1 ps. It might be higher threshold than that of the *c*-plane. This phenomenon is similar with GaN single crystal [19], which was also several times higher than *c*-plane irradiation. In the case of τ_{pulse} = 220 fs using double-pulse-trains, we were unable to apply the structural modification at the focal point even if the E_{pulse} is increasing until the surface has damaged (E_{pulse} ≈ 22 μJ). We changed the τ_{pulse} to enhance the light-matter interaction in longer time. The processing probability was in steady-state with τ_{pulse} at 1 ps as shown in Fig. 2, *a*. Figure 2, *b* shows the process window of E_{pulse} without surface damage from 1 to 20 μJ as a function of τ_{pulse} at 1 ps. Exceeding the 20 μJ would be surface damaged. The modified shape was like the inverse triangle. Both the modified width and height size were increased with increasing the E_{pulse} as shown in Fig. 2, *b*. We selected as a optimal condition for *a*-plane irradiation at τ_{pulse} = 1 ps, τ_{delay} = 3 ps and total E_{pulse} = 10 μJ, respectively. To investigate further topology of modified structure at the focal point, we did whole area processing using optimal condition. Then the *a*-plane sample was exfoliated to normal direction from focal point.

Cross-Sectional Analysis for Periodic Structure

Figure 3 shows the AFM topology and tilted FE–SEM analysis results of the structural modification in the propagation to the [0001] direction sample after dry-

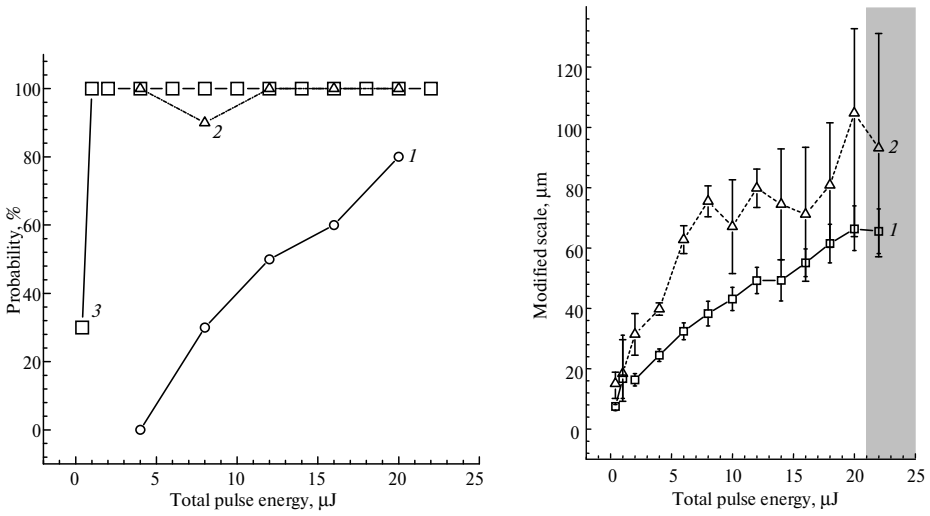

a *b*

Fig. 2. The probability of internal processing rate of (110) 4H–SiC as a function of the total pulse energy (*a*); the τ_{delay} set to minimum without overlap the each pulse to maximizing the light-matter efficiency; 500 fs/2 ps (*1*), 750 fs/2 ps (*2*), 1 ps/2 ps (*3*). The size of width (*1*) and height width (*2*) of the internal processing as a function of total pulse energy (*b*); the gray area since 22 μJ indicates surface damaged; the τ_{delay} between picosecond double pulse (τ_{pulse} = 1 ps) was set to 3 ps.

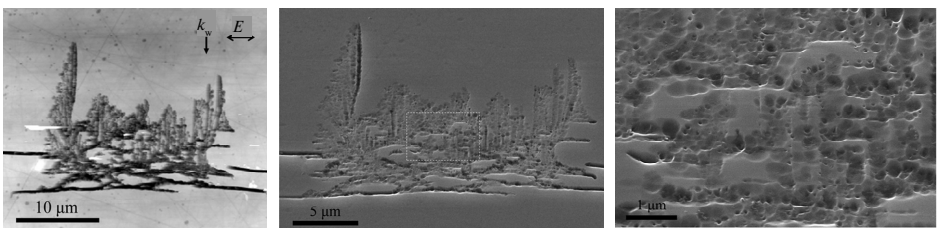

a *b* *c*

Fig. 3. Cross-sectional view of structural modifications in 4H–SiC (0001) plane after dry-etched using O_2/SF_6 for 30 s. AFM topology analysis (*a*), tilted FE-SEM image (*b*) and magnified image (*c*) from white-box in (*b*). The laser writing conditions by the double-pulse trains: E_{pulse} = (5 + 5) μJ, τ_{pulse} = 220 fs, τ_{delay} = 2 ps.

etched with double pulse train. The modified area was selectively etched about 100 nm. The cracks to the cleaver plane direction and nano voids of several tens nano-meter diameter were observed by O_2/SF_6 dry etching process for 30 s. It was convincing to think that considering the presence of amorphous Si and C previously confirmed by Raman analysis [23, 26], which was able to etch easily by SiC amorphization. Since the difference in density of dangling bond and reactivity on the surface causes a difference in etch rates between crystal and amorphous SiC [27]. Moreover, we confirmed that nano voids were formed in the modified region regardless of the pulse trains. In order to investigate the periodic nano structure, HRTEM analysis was performed with the sample vertically cut by focused-ion-beam. Figs. 4, *a–c* set and Figs. 4, *d–f* set are shows cross-sectional HRTEM with FFT analysis of the samples induced by single- and double pulse trains, respectively. There appears to be considerable difference of modified phase between single- and double-pulse-trains irradiation. In case of single pulse train, the FFT analysis on the area “b” (dark-contrast in Fig. 4, *a*) clearly shows as 4H–SiC crystal form (see Fig. 4, *b*). On the other hands, the other bright-contrast on the area “c”

shows as amorphous ring pattern. (see Fig. 4, *c*). We calculated the lattice spacing d from FFT analysis that the lattice spacing of (0004) *c*/4 (~ 0.244 nm) slightly compressed than that of non-stressed (~ 0.251 nm) lattice. In case of double pulse trains, the modified area was changed into poly-crystal. Figure 4, *e* FFT image shows diffraction pattern on the modified area of double pulse train sample that. There are two angle of $(2\,\bar{2}\,00)$ and $(2\,\bar{2}\,00)$* spots we found in the "region e". In particular, the spot reveal not only rotated *c*/4 and *a*/2 but also some alternative phases (d = 0.227, 0.316, 0.363, 0.498, 0.638 nm). We also found the elongated spot in the high contrast area (see inset of Fig. 4, *f*). The FWHM of diffraction spot intensity increased by 3 times from 0.30 to 0.98 nm^{-1} at the time of non-irradiation. We suppose such extended spots parallel to the axial direction caused by presence of axial defects. [28] According to literature, the lattice spacing for d = 0.316 and 0.638 nm are supposed to be graphite (0002) and (0001), respectively. We compared the lattice spacing d = 0.363 nm from previous report that the lattice constant is very similar with nano-crystal diamond ($d \approx 0.358$ nm) [29]. Based on the local heating and local high-pressure environment by ultrafast pulse laser, the nano diamond might be possible to create in the irradiated center. Furthermore, we also found the d = 0.498 nm forbidden Bragg scattering spot of (0002) 4H–SiC. We assumed that both (0001) graphite and (0002) 4H–SiC are apparently due to the double Bragg reflection occurring inside the disordered crystal [30]. The lattice spacing d = 0.227 nm is still unidentified structure phase. We also measured TEM-EDS analysis to investigate the element distribution change of silicon and carbon in the modified area. There are no significant change found the carbon distribution in both single- and double-pulse-train samples. On the other hand, although there were no significant change found the silicon distribution in the modified area, only silicon decreased in nano void.

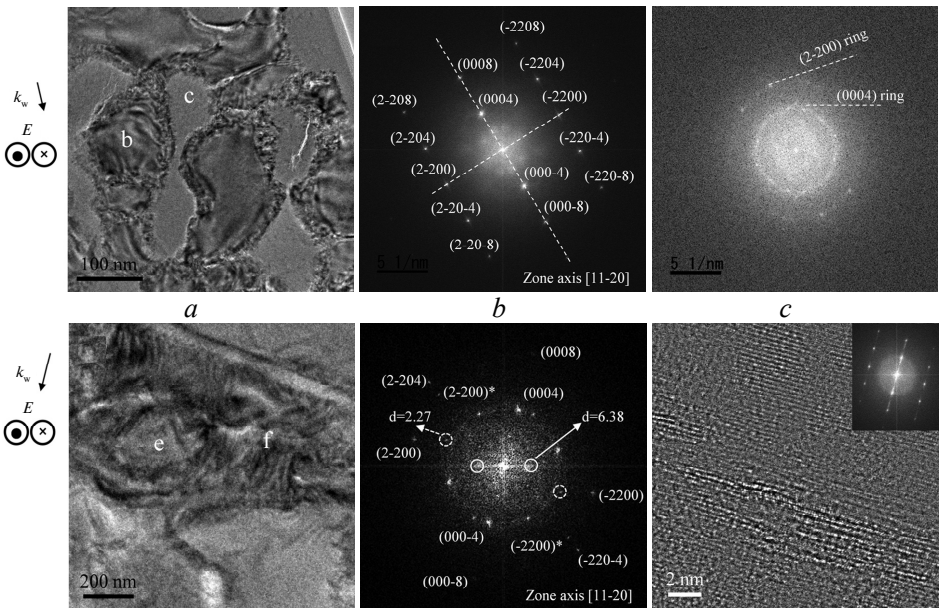

Fig. 4. Cross-sectional HRTEM images of the laser-written scanning induced by single- (*a*) and double-pulse-trains (*d*). FFT images of (*b*) and (*c*) are corresponding with region b and c in (*a*), respectively. The FFT result of (*e*) and (*f*) are corresponding with region e and f in (*d*). The laser writing conditions by the single-pulse trains: λ = 780 nm, E_{pulse} = 10 μJ, τ_{pulse} = 1 ps. The laser writing conditions by the double-pulse trains: E_{pulse} = (5 + 5) μJ, τ_{pulse} = 220 fs, τ_{delay} = 2 ps.

FE-SEM Analysis on the Exfoliated Surface

To investigate the modified structure in the wide area, we have also carried out the FE-SEM analysis on the vertically fractured sample surface. Figure 5, *a* shows SEM of the upper side surface of fractured sample induced by double-pulse-train irradiation. We can see there are periodic nano structure with beyond the diffraction limit. The periodic structure on the region A aligned in the direction parallel to the laser polarization direction. In addition, we also found polarization-independent structure; the shape is circular with direction to the laser-scan on the region B (see also Fig. 5, *b*). We suppose the modified region classified as two types of periodic structure; a curve type oriented in the scanning direction and a linear type oriented in the laser polarization direction. A similar phenomenon has reported in fused silica glass. Mcmillen et al. reported photo-induced periodic structures inside fused silica aligned with a circular or pseudo-random shape by azimuthal or radial polarization [31]. This is the first revealed phenomenon in the semiconductor instead of glasses. On the other hands, there are also much of large-scale (~ 100 nm) nano void on the fractured surface that diameter was bigger than cross-section TEM analysis (~ 20 nm) [20] (see Fig. 5, *c*). We assume that the difference of diameter is due to the different sample preparation method or 30 times higher (570 J/cm^2) fluence than other group (17.7 J/cm^2). Note that such three structures also observed on the fractured surface induced by single-pulse-train irradiation. We speculated these characteristic distributions can be accounted as follow. If the laser applied in the focal depth, a periodic structure formed as a direction parallel to the laser polarization by light-matter interaction at the upper focal depth (region A). At the same time, some complicated processes such as the self-focusing due to Kerr effect and self-defocusing by plasma generation, dissociation of Si–C bonding, defect, and local-strain, also can occur during irradiation when the peak power of laser is above the critical point (P_{cr}) at the focal depth. These might be allowing periodic structure forming as polarization-independently (region B).

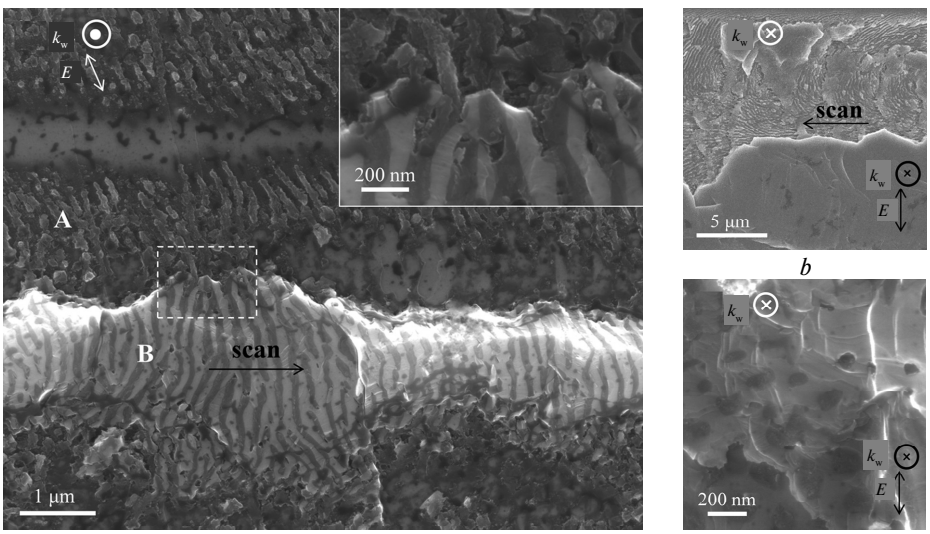

Fig. 5. FE-SEM image of exfoliated 4H–SiC surface induced by double-pulse-trains: top-surface (*a*), bottom-surface (*b*–*c*). Inset shows magnified image of the white box area in (*a*). The laser writing conditions by the double-pulse trains: E_{pulse} = (5 + 5) μJ, τ_{pulse} = 220 fs, τ_{delay} = 1 ps.

Based on the inhomogeneous nano plasma model [32, 33], the period of nanostructures in matter is defined as follow:

$$\Lambda = \lambda/2n,$$

where λ is the laser wavelength, n is the refractive index of material. We obtained the interval of periodic structure is 154 nm at the wavelength of 800 nm as shown in Fig. 6. The interval distributed in the range from 130 to 170 nm, which value agrees with the calculation. In addition, there are no doubled-interval (~ 300 nm) of periodic structures found on the fractured sample, which originated by second order wavelength [20]. On the contrary, occasionally a half interval (60–80 nm) structures was observed in the polarization-independent surface. While the high-spatial-frequency-LIPSS (HSFL) on the surface phenomenon has well-investigated [34, 35], such similar structure in the matter is relatively under-investigated. In order to investigate the alignment dependence of the periodic structure with crystal orientation, we prepared not only *c*-plane fractured sample but also *a*-plane fractured one. Figure 7 shows bottom side of fractured *a*-plane induced by double pulse trains irradiation. The alignment of periodic structure also arranged with the direction parallel to the laser polarization. This indicate that alignment of periodic structure is independent with crystal orientation. The interval of periodic structure was about 150 nm as well as *c*-plane.

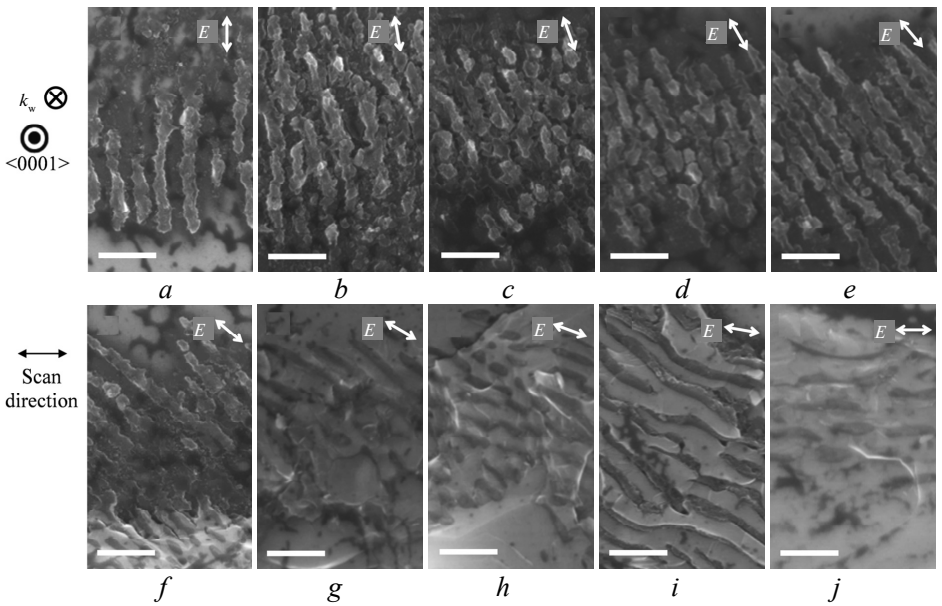

Fig. 6. FE-SEM images of the periodic nano structure on the exfoliated surface: laser polarization E = 0 (*a*), 10º (*b*), 20º (*c*), 30º (*d*), 40º(*e*), 50º (*f*), 60º (*g*), 70º (*h*), 80º (*i*), 90º (*j*). The scale bar indicates 500 μm. The laser writing conditions by the double-pulse trains: E_{pulse} = (5 + 5) μJ, τ_{pulse} = 220 fs, τ_{delay} = 1 ps.

CONCLUSIONS

We have demonstrated the self-organized structure inside 4H–SiC using femtosecond pulse laser with double-pulse-train technique. In the case of strong fluence, the periodic nano structure inside 4H–SiC is classified into two categories of the polarization-dependent and polarization-independent. In particular, alignment of the periodic structure is in the direction independently from crystal orienta-

tion. It was shown that the some other phases were found in the modified area instead of 4H–SiC poly-crystal or amorphous. Moreover, the transformed structure is not observed significant change of the elemental distribution.

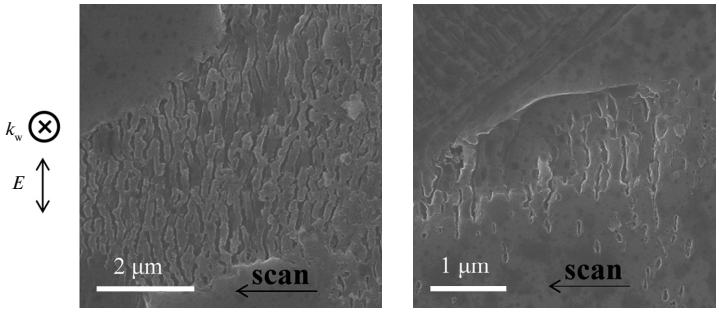

Fig. 7. FE-SEM image of the periodic nano structure on the bottom-surface exfoliated from *a*-plane 4H-SiC. Each figure was captured on the individual place, respectively. The arrow in the figure indicate scan-direction. The laser writing conditions by the double-pulse trains: E_{pulse} = (5 + 5) μJ, τ_{pulse} = 1 ps, τ_{delay} = 3 ps.

This work was partially supported by JSPS KAKENHI (No. 16K13929), Cross-Ministerial Strategic Innovation Promotion (SIP) Program.

Фотоіндукована періодична наноструктура всередині 4H–SiC була індукована фемтосекундним подвійним імпульсом. Вирівнювання періодичної структури відбувалося в напрямку, незалежному від орієнтації кристала. Зокрема, аналіз FE-SEM показав, що періодичну структуру на тріщинуватій поверхні можна розділити на дві категорії: поляризаційно-залежної та незалежної від поляризації.

***Ключові слова**: 4H–SiC, періодична наноструктура, фемтосекундний лазер, подвійний імпульс, зміна фази, напівпровідник.*

Фотоиндуцированная периодическая наноструктура внутри 4H–SiC была индуцированна фемтосекундным двойным импульсом. Выравнивание периодической структуры происходило в направлении, независимом от ориентации кристалла. В частности, анализ FE-SEM показал, что периодическую структуру на трещиноватой поверхности можно разделить на две категории: поляризационно-зависимой и независимой от поляризации.

***Ключевые слова**: 4H–SiC, периодическая наноструктура, фемтосекундный лазер, двойной импульс, изменение фазы, полупроводник.*

1. *Ikeno J., Y. Tani, Fukutani A., Sato H*. Development of chipping-free dicing technology applying electrophoretic deposition of ultrafine abrasives // Ann. CIRP. – 1991. – **40**, N 1. – P. 351–354.
2. *Cho I. H., Jeong S. C., Park J. M., Jeong H. D.* The application of micro-groove machining for the model of PDP barrier ribs // J. Mater. Process. Technol. – 2001. – **113**, N 1. – P. 355–359.
3. *Peng W., Xu X. F., Zhang L. F*. Improvement of a dicing blade using a whisker direction-controlled by an electric field // J. Mater. Process. Technol. – 2002. – **129**, N 1. – P. 377–379.
4. *Lee S. B., Tani Y., Enomoto T., Sato H.* Development of a dicing blade with photopolymerizable resins for improving machinability // Ann. CIRP. – 2005. – **54**, N 1. – P. 293–296.
5. *Koch W., Endrös A. L., Franke D., Häßler C., Kalejs J. P., Möller H. J.* Handbook of Photovoltaic Science and Engineering. – Hoboken, NJ: Wiley, 2002. – 2nd ed. – Chap. 6.4.
6. *Cioccio L. Di, Letertre F., Tiec Y. Le, Papon A. M., Jaussaud C., Bruel M.* Silicon carbide on insulator formation by the Smart-Cut®process // Mater. Sci. Eng. B. – 1997. – **46**, N 1. – P. 349–356.

7. *Lee J. H., Bargatin I., Park J., Milaninia K. M., Theogarajan L. S., Sinclair R., Howe R. T.* Smart-cut layer transfer of single-crystal SiC using spin-on-glass // J. Vac. Sci. Technol. B. – 2012. – **30**, N 4, art. 042001.
8. *Amarasinghe V. P., Wielunski L., Barcz A., Feldman L. C., Celler G. K.* Properties of H+ implanted 4HSiC as related to exfoliation of thin crystalline films // ECS J. Solid State Sci. Technol. – 2014. – **3**, N 3. – P. 37–42.
9. *Fukuyo F., Fukumitsu K., Uchiyama N.* The stealth dicing technologies and their application // Proc. 6th Int. Symp. "LPM2005", Williamsburg, USA, 4–8 Apr., 2005.
10. *Ohmura E., Fukuyo F., Fukumitsu K., Morita H.* Internal modified-layer formation mechanism into silicon with nanosecond laser // JAMME. – 2006. – **17**, N 1. – P. 381–384.
11. *Sales* Engineering Department, Dicing technologies for SiC, (DISCO Technical Review Mar. 2016), https://www.disco.co.jp/eg/solution/technical_review/pdf/TR16-05_eg.pdf?20160620.
12. *Hirata K., Takahashi K., Nishino Y.* JP patent 2016-111144, 20 July 2016, H01L 21/304.
13. *Disco* Cooperation, KABRA® Process, https://www.disco.co.jp/kabra/index_eg.html.
14. *Davis K. M., Miura K., Sugimoto N., Hirao K.* Writing waveguides in glass with a femtosecond laser // Opt. Lett. – 1996. – **21**, N 21. – P. 1729–1731.
15. *Shimotsuma Y., Kazansky P.G., Qiu J., Hirao K.* Self-organized nanogratings in glass irradiated by ultrashort light pulses // Phys. Rev. Lett. – 2003. – **91**, N 24, art. 247405.
16. *Shimizu M., Shimotsuma Y., Sakakura M., Yuasa T., Homma H., Minowa Y., Tanaka K., Miura K., Hirao K.* Periodic metallo-dielectric structure in diamond // Opt. Express. – 2009. – **17**, N 1. – P. 46–54.
17. Shimotsuma Y., Hirao K., Qiu J., Kazansky P. G. Nano-modification inside transparent materials by femtosecond laser single beam // Mod. Phys. Lett. B. – 2005. – **19**, N 5. – P. 225–238.
18. *Ishikawa Y., Shimotsuma Y., Kaneta A., Sakakura M., Nishi M., Miura K., Hirao K., Kawakami Y.* Fabrication of photo-induced microstructure embedded inside ZnO crystal // Proc. SPIE. – 2012. – **8243**. – P. 82430N.
19. *Sei T., Shimotsuma Y., Sakakura M., Miura K.* Self-assembled nanostructures inside indirect bandgap semiconductor by using IR femtosecond double-pulses // J. Laser Micro/Nanoeng. – 2016. – **11**, N 1. – P. 76-80.
20. *Okada T., Tomita T., Matsuo S., Hashimoto S., Ishida Y., Kiyama S., Takahashi T.* Formation of periodic strained layers associated with nanovoids inside a silicon carbide single crystal induced by femtosecond laser irradiation // J. Appl. Phys. – 2009. – **106**, N 5, art. 054307.
21. *Sei T., Shimotsuma Y., Sakakura M., Miura K.* Self-assembled nanostructures inside indirect bandgap semiconductor by using IR femtosecond double-pulses // J. Laser Micro/Nanoeng. – 2016. – **11**, N. 1. – P. 76–80.
22. *Mori M., Shimotsuma Y., Sei T., Sakakura M., Miura K., Udono H.* Tailoring thermoelectric properties of nanostructured crystal silicon fabricated by infrared femtosecond laser direct writing // Phys. Status Solidi. A. – 2015. – **212**, N 4. – P. 715–721.
23. *Kim E., Shimotsuma Y., Sakakura M., Miura K.* 4H–SiC wafer slicing by using femtosecond laser double-pulses // Opt. Mater. Express. – 2017. – **7**, N 7. – P. 2450–2460.
24. *Sugioka K., Iida M., Takai H., Micorikawa K.* Efficient microwelding of glass substrates by ultrafast laser irradiation using a double-pulse train // Opt. Lett. – 2011. – **36**, N 14. – P. 2734–2736.
25. *Biedermann E.* The optical absorption bands and their anisotropy in the various modifications of SiC // Solid State Commun. – 1965. – **3**, N 10. – P. 343–346.
26. *Yamamoto M., Deki M., Takahashi T., Tomita T., Okada T., Matsuo S., Hashimoto S., Yamaguchi M., Nakagawa K., Uehara N., Kamano M.* Raman Spectroscopic Stress Evaluation of Femtosecond-Laser-Modified Region Inside 4H-SiC // Appl. Phys. Express. – 2010. – **3**, art. 016603.
27. *Pearton S. J.* Processing of 'Wide Band Gap Semiconductors (Materials and Processing Technology). – Norwich, NY: William Andrew, 2000. – 1st ed. – Chap. 4.2.
28. *Wang H. B., Ma F., Li Q. Q., Dong C. Z., Ma D. Y., Wang H. T., Xu K. W.* Synthesis and stress relaxation of ZnO/Al-doped ZnO core–shell nanowires // Nanoscale. – 2013. – **5**. – P. 2857–2863.
29. *Yur'ev G.S., Dolmatov V. Yu.* X-Ray Diffraction study of detonation nanodiamonds // J. Superhard Mater. – 2010. – **32**, N 5. – P. 311–328.
30. *Fultz B., Howe J. M.* Transmission Electron Microscopy and Diffractometry of Materials. – Heidelberg, Berlin: Springer, 2013. – 4th ed. – Chap 6.4.

31. *McMillen B., Bellouard Y.* On the anisotropy of stress-distribution induced in glasses and crystals by non-ablative femtosecond laser exposure // Opt. Express. – 2015. – **23**, N 1. – P. 87–100.
32. *Rajeev P. P., Gertsvolf M., Hnatovsky C., Simova E., Taylor R. S., Corkum P. B., Rayner D. M., Bhardwaj V. R.* Transient nanoplasmonics inside dielectrics // J. Phys. B: At. Mol. Opt. Phys. – 2007. – **40**. – P. S273–S282.
33. *Taylor R.S., Hnatovsky C., Simova E.* Applications of femtosecond laser induced self-organized planar nanocracks inside fused silica glass // Laser & Photon. Rev. – 2008. – **2**, N 1–2. – P. 26–46.
34. *Tomita T., Kinoshita K., Matsuo S., Hashimoto S.* Effect of surface roughening on femtosecond laser-induced ripple structures // Appl. Phys. Lett. – 2007. – **90**, art. 153115.
35. *Bonse J., Krüger J., Höhm S., Rosenfeld A*. Femtosecond laser-induced periodic surface structures // J. Laser Appl. – 2012. – **24**, N 4, art. 042006.

Received 02.11.17